

# Rating Reduction and Optimized DC-Link Voltage of the HPQC in Co-Phase Traction Power System

M. Habibolahzadeh\* and A. Jalilian\*<sup>\*,\*\*</sup>(C.A.)

**Abstract:** Electric traction trains are huge non-linear single-phase loads influencing adversely on power quality parameters on the grid side. Hybrid power quality conditioner (HPQC) has been utilized to compensate current unbalance, harmonics, and low power factor in the co-phase traction system simultaneously. By incrementing the traction load, the rating of the HPQC increases and may constraints its application. In this paper, a C-type filter is designed to compensate for some part of the load reactive power while the HPQC compensates the remaining part of the load reactive power. Hence, the capacity of the HPQC is reduced in full compensation (FC) mode compared to the conventional configuration. The satisfactory performance of the HPQC is associated with its DC-link operating voltage. Therefore, the Genetic algorithm (G.A) is adopted to optimize the DC-link voltage performance. Simulation verifications are performed to illustrate the usefulness of the proposed configuration. The simulation results show an 18.86% reduction in the rating of the HPQC with optimized DC-link voltage.

**Keywords:** HPQC, C-Type Filter, Co-Phase, Power Quality.

## 1 Introduction

RAILWAY electrification has been implemented in many countries due to its high-capacity, high-speed, and more reliability in transportation systems [1, 2]. However, there are significant power quality problems in electric railway systems, e.g., three-phase voltage and current unbalance, low grid power factor (PF), low total harmonic distortion (THD), harmonic resonance and malfunction of relays, the high temperature of transformers and motors [2, 3]. The acceptable values of the power quality parameters have been provided by the IEEE standards for various power supply systems [4]. To overcome these issues, many methods have been explored and investigated. Among them, traction transformers such as V/v, Scott, Leblanc,

Modified Woodbridge, and ABTT are connected to the power supply to reduce the unbalanced system [5-8]. Unfortunately, because of the variable nature of the traction loads, the unbalanced currents would be remained and may not be compensated completely. Other passive devices, e.g., single tuned, LC, and its derivatives are used to compensate for the harmonic currents generated by the trains. A C-type filter is another passive filter that is used in the electric railway to mitigate high-order harmonics caused by the train converters [9-11]. The parameters of the passive filters do not change when the load varies, while active filters generate compensation currents with power-electronic based switches dynamically. There are many proposed active filters in prior studies. SVC [12] and STATCOM [13] have been investigated, but the harmonic distortions during their compensation method remain. The next generation of static converters is then introduced based on FACTS devices. One of them is widely used in the electrified railway system is the Railway static Power Conditioner (RPC) [14], which can compensate three considerable power quality problems (PF, harmonics, unbalanced system) simultaneously. Various types of RPC, e.g., Active Power Quality Conditioner (APQC) [15], Half-Bridge Railway Power Conditioner (HBRPC) [16], Hybrid Power Quality Conditioner (HPQC) [17], are then

Iranian Journal of Electrical and Electronic Engineering, 2021.  
Paper first received 06 November 2018, revised 17 August 2020, and accepted 04 September 2020.

\* The authors are with the Department of Electrical Engineering, Iran University of Science and Technology (IUST), Tehran, Iran.  
E-mails: [m\\_habibolahzadeh@elec.iust.ac.ir](mailto:m_habibolahzadeh@elec.iust.ac.ir) and [jalilian@iust.ac.ir](mailto:jalilian@iust.ac.ir).

\*\* The author is with the Centre of Excellence for Power System Automation and Operation, Iran University of Science and Technology (IUST), Tehran, Iran.

Corresponding Author: A. Jalilian.  
<https://doi.org/10.22068/IJEEE.17.2.1377>

explored. The main problem of the RPC is the high associated capacity to the converters and hence cost limitations. Many methods are used to decrease the rating of the converters. A TSC as the secondary device has been used with the RPC to reduce its rating [18]. These low rating devices could compensate a part of the compensation currents. The combination of magnetic SVC and RPC has been proposed by Chen and *et al.* [19]. An integration of APQC and SVC was introduced in [20]. In addition, the LC branch in the output of one phase of the RPC is added to reduce the DC-link voltage with similar compensation performances [21, 22]. These methods need an integrated control strategy for main and auxiliary compensators and increase the complexity of the control unit [4]. The HPQC structure is then utilized in a co-phase traction system with satisfactory compensation [23, 24]. As described above, a C-type filter performs as high-impedance for low-order harmonics as well as it can be provided the reactive compensation for the traction loads. In this paper, using a C-type filter in the HPQC co-phase traction system is introduced and investigated. The compensator performance is extremely related to its operating voltage. A PI controller is mostly used to correct the DC-link voltage via the trial and error (T&E) method [25]. To optimize the DC-link voltage of the HPQC, the Genetic algorithm (G.A) is applied to the control system for regulation of PI controller parameters. The part of the reactive power compensation of the HPQC is injected by the C-type filter. Therefore, the load PF is corrected by the C-type filter and the capacity of the HPQC is then reduced compared to the conventional structure. In Section 2 the proposed configuration is described. In Section 3, the principle of compensation method with C-type filter and its capacity calculation are analyzed. The control strategy based on instantaneous power theory (PQ theory) is introduced in Section 4. The simulation results are performed using MATLAB/Simulink to show the usefulness of the proposed scheme. Finally, a conclusion is made in Section 5.

## 2 The Proposed Configuration in the Co-Phase System

In Fig. 1, the proposed HPQC configuration with a C-type filter is illustrated. In the co-phase traction system, the neutral sections between the output supply feeders are omitted [26]. Hence, the train can reach its maximum speed in the railroad system. The traction substation consists of two single transformers. Three-phase voltages transform into two output phases with 60 degrees phase differences.

The traction loads are connected to ac phase while bc phase remains unloaded. The HPQC includes two back-to-back converters with four legs, in which each leg has

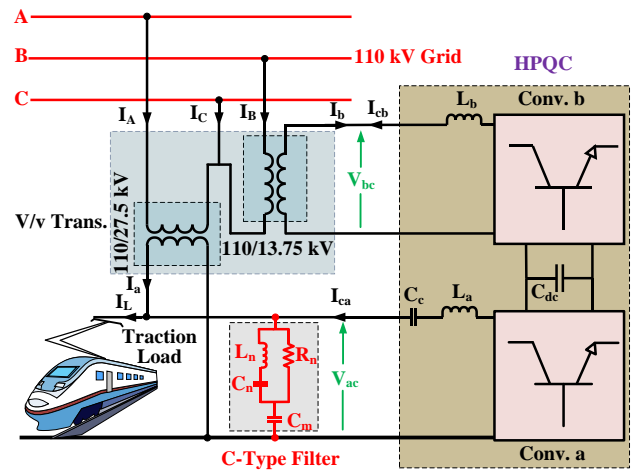


Fig. 1 Proposed of the HPQC with C-type filter.

two IGBT switches. The LC branch is connected to ac phase for DC-link voltage reduction. The two converters of the HPQC operate in the same DC-link voltage [22]. By using the C-type filter in the output of ac phase, the load reactive power compensation is provided, which is described in the next section.

### 2.1 Compensation Principles of the HPQC With the C-Type Filter

A vector diagram of the proposed configuration without any compensation is depicted in Fig. 2(a). The secondary currents of the transformer without compensation considering load current ( $i_L$ ) are as follows:

$$\begin{cases} i_a = i_L \\ i_b = 0 \end{cases} \quad (1)$$

The grid-side currents can be easily obtained concerning the transformer turn ratio ( $k_2=1/k_1=27.5/110$ ) as follows:

$$\begin{cases} i_A = k_2 i_a \\ i_B = i_b = 0 \\ i_C = -i_A = -k_2 i_a \end{cases} \quad (2)$$

By using Fortescue’s method of symmetrical components, the negative sequence current (NSC) index is obtained as follows:

$$\begin{bmatrix} I_0 \\ I_+ \\ I_- \end{bmatrix} = \frac{1}{3} \begin{bmatrix} 1 & 1 & 1 \\ 1 & a & a^2 \\ 1 & a^2 & a \end{bmatrix} \begin{bmatrix} I_A \\ I_B = 0 \\ I_C = -I_A \end{bmatrix} \quad (3)$$

$$\begin{bmatrix} I_0 \\ I_+ \\ I_- \end{bmatrix} = \frac{1}{3} \begin{bmatrix} 0 \\ (1-a^2)I_A \\ (1-a)I_A \end{bmatrix}, \quad \frac{I_-}{I_+} = \frac{(1-a)}{(1-a^2)} \rightarrow \left| \frac{I_-}{I_+} \right| = 1 \quad (4)$$

Regarding (4), grid side currents unbalance is beyond allowable constraints. The NSC index is practically close to 1 with an unloaded phase. The higher value of NSC can be adversely affected on voltage unbalance in a low short-circuit power railway system. Therefore, the system should be compensated to overcome the unbalanced system properly. The vector diagram of a compensation strategy using HPQC in FC method with the C-type filter is shown in Fig. 2(b). The ac and bc phase compensation currents are described as  $i_{ca}$  and  $i_{cb}$ . In this section, these currents are obtained in full compensation method (unity PF, harmonic-free and balanced system) [21]. The load current is divided into two components of the fundamental and harmonic frequencies as follows:

$$i_L = i_{L1p} + i_{L1q} + i_{Lh} \quad (5)$$

in which,  $i_{L1p}$ ,  $i_{L1q}$ , and  $i_{Lh}$  refer active, reactive, and harmonic load currents, respectively.

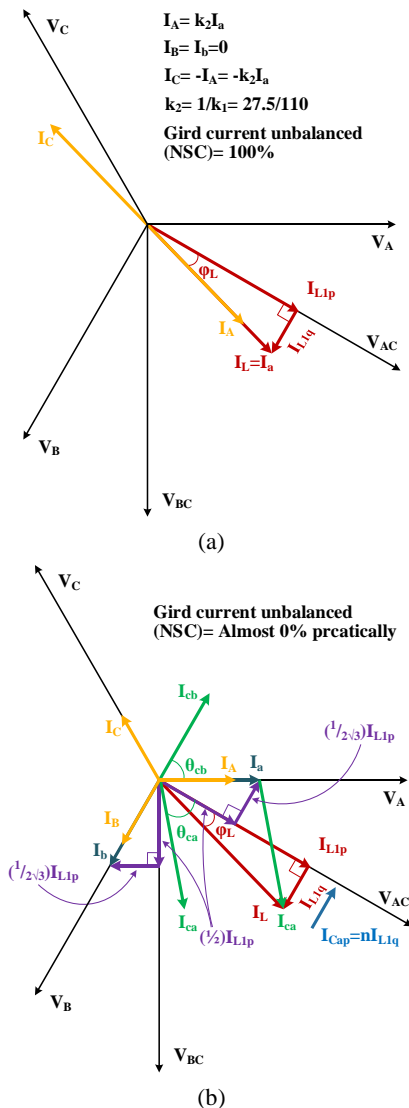


**Fig. 2** Vector diagram of the proposed configuration: a) Without compensation and b) Using HPQC and C-type filter.

A C-type filter has no fundamental losses compared to other passive filters. Therefore, it can be used to compensate for high-order harmonics and load reactive power in the co-phase traction system. The effect of the load reactive power compensation is considered by the C-type filter. Through the vector diagram shown in Fig. 2(b) and the following mathematical relations, a reduction in the HPQC capacity as well as decreasing in NSC index are verified. The capacitive current ( $I_{Cap}$ ) is obtained as follows:

$$i_{Cap} = \sqrt{2} I_{Cap} \cos(\omega t - 30^\circ) \quad (6)$$

The capacitive current to the reactive load current ratio is defined as  $n$  factor that satisfies:

$$\frac{I_{Cap}}{I_{L1q}} = n, \quad 0 < n < 1 \quad (7)$$

By substituting (7) into (6), the new reactive load current is achieved as follows:

$$i_{L1q\_new} = \sqrt{2}(n-1)I_{L1q} \cos(\omega t - 30^\circ) < i_{L1q} \quad (8)$$

The part of the load reactive current is compensated by the C-type filter while the load active current remains constant. The new compensation currents related to load PF are obtained as follows:

$$\begin{cases} I_{ca} = I_{L1} \sqrt{\left[ (1-n) \sin(a \cos(PF_L)) + \frac{1}{2\sqrt{3}} PF_L \right]^2 + \left( \frac{1}{2} PF_L \right)^2} \\ I_{cb} = \frac{1}{2} I_{L1} PF_L \sqrt{1 + \left( \frac{1}{\sqrt{3}} \right)^2} = \frac{1}{\sqrt{3}} I_{L1} PF_L \end{cases} \quad (9)$$

It is observed that  $i_{ca}$  is reduced while  $i_{cb}$  has no change in the presence of the C-type filter. The compensation current phase angles ( $\theta_{ca}$  and  $\theta_{cb}$ ) are defined as:

$$\begin{cases} \theta_{ca} = a \tan \left( \frac{1}{\sqrt{3}} + 2(1-n) \tan(\varphi_L) \right) \\ \theta_{cb} = a \tan \left( \frac{\frac{1}{2} I_{L1p}}{\frac{1}{2\sqrt{3}} I_{L1q}} \right) = 60 \end{cases} \quad (10)$$

The  $\theta_{ca}$  gets a bit smaller, while the  $\theta_{cb}$  remains constant. After full compensation,  $I_a$  and  $I_b$  are in phase  $V_A$  and  $V_B$ , respectively. Hence, the primary transformer currents and grid NSC index can be calculated as follow:

$$\begin{cases} i_A = k_2 i_a \\ i_B = k_2 i_b \\ i_C = -(i_A + i_B) = -k_2 (i_a + i_b) \end{cases} \quad (11)$$

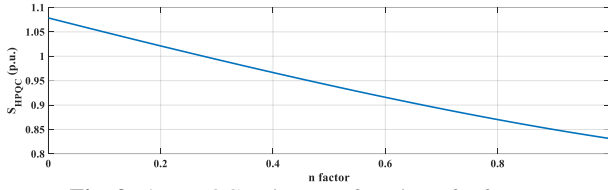


Fig. 3 The HPQC rating as a function of n factor.

Regarding (11) and Fig. 2(b), the grid-side currents are symmetric three-phase currents reaching NSC index to 1. Therefore, the system unbalance is fully compensated in this method. The operating voltage of the HPQC is considered as 0.8 p.u. of the  $V_{ac}$  supply phase [24]. The  $\theta_{ca}$  variations are negligible in the range of  $0.8 \leq PF_L \leq 0.9$  and do not affect the DC-link voltage. Therefore, the output operation voltages of the converters are the same. The rating of the HPQC is reduced with the C-type filter compared to the conventional structure. Fig. 3 shows the reduced HPQC rating as a function of n factor. As can be seen, by increasing the n factor, the reduction of the HPQC rating is further increased. However, to prevent overcompensation, the lower n values are appropriate. The reduction of the HPQC rating using the C-type filter is as follows:

$$\left\{ \begin{array}{l} I_{ca\_f\_new} < I_{ca\_f}, I_{cb\_f\_new} = I_{cb\_f} \\ \frac{(I_{ca\_f\_new} + I_{cb\_p})}{(I_{ca\_f} + I_{cb\_f})} = k < 1 \\ V_{dc} = cte \quad \text{for} \quad 0.8 < PF_L < 0.9 \\ \frac{S_{HPQC\_C\_Filter}}{S_{HPQC}} = \frac{V_{conv.a} (I_{ca\_f\_new} + I_{cb\_f\_new})}{V_{conv.a} (I_{ca\_f} + I_{cb\_f})} = k < 1 \end{array} \right. \quad (12)$$

## 2.2 C-Type Filter Design in Co-Phase Traction System

The simplified circuit of the C-type filter is illustrated in Fig. 4, in which,  $X_{eq}$  is the equivalent of the system impedance seen by the filter. The C-type filter has no fundamental losses compared to other passive filters. This is the main advantage of this filter that distinguishes it from other ones. The capacitor  $C_m$  is so designed for load reactive power compensation. To avoid over-compensation, the reactive power compensation by the filter should be lower than the load reactive power consumption. Hence, the PF value and the MVA of a unit train are assumed 0.9 and 5 MVA for the filter design, respectively.  $C_m$  is obtained as:

$$\begin{aligned} Q_{Cap} = S_{load} \sqrt{1 - PF_L^2} \rightarrow X_{Cm} &= \frac{V_{ac}^2}{Q_{Cap}} \\ \rightarrow C_m &= \frac{1}{2\pi f_{grid} X_{Cm}} \end{aligned} \quad (13)$$

where  $f_{grid}$  is the fundamental grid frequency.  $C_n$  and  $L_n$

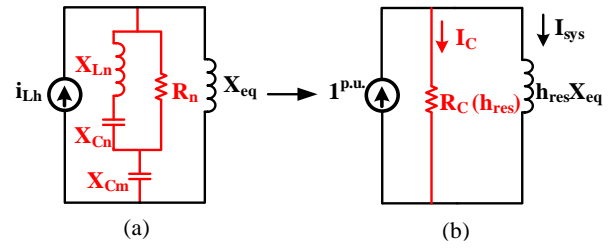


Fig. 4 The C-type filter: a) The topology of the C-type filter and b) The equivalent of the C-type filter at the tuned frequency.

are adjusted at the fundamental frequency ( $X_{Ln} = X_{Cn}$ ), bypassing  $R_n$  to inject reactive power with no filter loss.

The value of  $C_m$  is 9.1734  $\mu\text{F}$  for 27.5 kV and 50 Hz power supply system. Moreover, this high-pass filter is tuned at the high-frequency order, and  $R_n$  with  $C_m$  bypasses the parallel  $LC_n$  branch at high-frequencies. Consequently, the C-type filter acts as a first-order filter at high-order frequencies. Regarding Fig. 4(a), the filter impedances at high-order frequencies (h) are as follows:

$$\left\{ \begin{array}{l} X_{Ln}(h) = h\omega_1 L_n = hX_{Ln} \\ X_{Cn}(h) = \frac{1}{h\omega_1 C_n} = \frac{1}{h} X_{Cn} \\ X = X_{Ln} = X_{Cn}, X_{Cm}(h) = \frac{1}{h} X_{Cm} \end{array} \right. \quad (14)$$

The impedance of the C-type filter is simply derived as:

$$\left\{ \begin{array}{l} R_C(h) = \frac{R_n \left[ X \left( h - \frac{1}{h} \right) \right]^2}{R_n^2 + \left[ X \left( h - \frac{1}{h} \right) \right]^2} \\ X_C(h) = \frac{R_n^2 \left[ X \left( h - \frac{1}{h} \right) \right]^2}{R_n^2 + \left[ X \left( h - \frac{1}{h} \right) \right]^2} - \frac{1}{h} X_{Cm} \end{array} \right. \quad (15)$$

At tuned  $h_{res}$  frequency,  $X_C(h_{res}) = 0$  and the equivalent of the C-type filter is considered as a pure resistance  $R_C(h_{res})$  shown in Fig. 4(b). The maximum permissible value of the injected current to the grid-side power supply at  $h_{res}$  frequency is defined as  $I_{sys}$ , which could be obtained as:

$$\begin{aligned} I_{sys}^{p.u.} &= \frac{R_C(h_{res})}{\sqrt{R_C^2(h_{res}) + (h_{res} X_{eq})^2}} \\ \rightarrow R_C(h_{res}) &= \frac{h_{res} X_{eq}}{\sqrt{\left( \frac{1}{I_{sys}^{p.u.}} \right)^2 - 1}} \end{aligned} \quad (16)$$

The  $R_n$  and  $X$  can be easily calculated according to (16)

and (17) at tuned  $h_{res}$  as follows:

$$\left\{ \begin{array}{l} R_n = \frac{R_C^2 (h_{res}) + \left[ \frac{X_{Cm}}{h_{res}} \right]^2}{R_C (h_{res})} \\ X = \frac{R_C^2 (h_{res}) + \left[ \frac{X_{Cm}}{h_{res}} \right]^2}{\left( \frac{X_{Cm}}{h_{res}} \right) \left( h_{res} - \frac{1}{h_{res}} \right)} - \frac{1}{h} X_{Cm} \end{array} \right. \quad (17)$$

The C-type filter is tuned as a system resonance frequency (23.3pu based on [11]). Assuming  $I_{sys} = 0.3$  p.u., the C-type filter parameters are listed in Table 1. The extra resonance frequency point ( $f_{extra.res}$ ) introduced at the cross point of the filter and system impedances is suppressed by the  $R_n$  [11]. The switching frequency of the train PWM converters is assumed to be around 4.5 kHz. Then the value of  $R_n$  is so designed that will be satisfied:

$$\left\{ \begin{array}{l} X_{LCn(at f_{extra.res})} \leq R_n \leq X_{LCn(at f_{switching})} \\ 9.56\Omega \leq R_n \leq 57.61\Omega \rightarrow R_n = 40\Omega \end{array} \right. \quad (18)$$

### 3 The Control Strategy of the HPQC

The control diagram of the HPQC in the FC method is presented in Fig. 5. The modified instantaneous PQ theory in the co-phase system is applied to calculate the instantaneous active and reactive power ( $p$  and  $q$ ) of the traction load. These powers are obtained by using Clark transformer as given in (19), in which  $V_{acd}$  and  $I_{Ld}$  are the 90 degrees lag of the  $V_{ac}$  and  $I_{Ld}$ , respectively.

$$\left\{ \begin{array}{l} p = V_{ac} i_{Ld} + V_{acd} i_{Ld} \\ q = V_{acd} i_{Ld} - V_{ac} i_{Ld} \end{array} \right. \quad (19)$$

The complexity in the control strategy is not required using the C-type filter. Some part of the load reactive power is compensated by the C-type filter, while the HPQC compensates the remaining part. The active power  $p$  can be divided into two parts, one is defined as  $p_{dc}$ , which shows the fundamental average active power part, and the other is  $p_{ac}$ , which corresponds to the oscillating power part, including harmonics and reactive power.

$$p = p_{dc} + p_{ac} \quad (20)$$

During compensation, active and reactive power compensation  $p_{ca}$  and  $q_{ca}$  are injected to  $V_{ac}$  phase by the converter "a" while the required compensation active and reactive powers for converter "b" are absorbed from the  $V_{bc}$  phase. These required compensation power can be calculated according to (21).

$$\left\{ \begin{array}{l} p_{ca} = \frac{1}{2} p_{dc} + p_{ac} \\ q_{ca} = \frac{1}{2\sqrt{3}} p_{dc} + \begin{cases} q, CTF OUT \\ q - q_{Cm}, CTF IN \end{cases} \\ p_{cb} = -\frac{1}{2} p_{dc} - p^* \\ q_{cb} = -\frac{1}{2\sqrt{3}} p_{dc} \end{array} \right. \quad (21)$$

Consequently, the HPQC can compensate the power quality requirement on the grid side. To maintain the DC-link stable, converter "b" is used to adjust DC common voltage and provides corresponding power  $p^*$ . However, the suitable performance of the HPQC is highly related to the DC-link voltage. In most cases, the control parameters of the PI controller ( $k_p$  and  $k_i$ ) are adjusted via T&A method. To maintain the DC-link voltage more reliable, GA optimization is implemented to achieve the optimum values of  $k_p$  and  $k_i$ . When these parameters are tuned precisely, the performance of the HPQC and the dynamic response of the DC-link voltage are improved. The multi-objective function is considered to optimize the DC-link voltage as follows:

$$\left\{ \begin{array}{l} O.F = w_1 J_1(V_{dc}) + \frac{w_2}{N} J_2(V_{dc}) \dots \\ \dots = 0.8 \left( \frac{1}{T} \int_T (V_{dc} - V_{dc.ref})^2 \right) + \frac{0.2}{5} (\max(V_{dc}) - \min(V_{dc})) \end{array} \right. \quad (22)$$

The DC-link voltage ripple and the differences between the maximum and minimum value of the DC-link voltage are defined as  $J_1(V_{dc})$  and  $J_2(V_{dc})$ ; respectively. The DC-link reference voltage should be appropriately followed by the actual DC-link voltage. Therefore, the value of  $w_1$  (weighted coefficient of  $J_1(V_{dc})$ ) is so selected to be greater than  $w_2$  (weighted coefficient of  $J_2(V_{dc})$ ). Since the allowable of the maximum and minimum value of the DC-link should be an allowable range, the normalized factor is assumed to be 5 here. Consequently, The  $k_p$  and  $k_i$  parameters are obtained via both methods and tabulated in Table 1.

The reference compensation currents,  $i_{ca}^*$ , and  $i_{cb}^*$  are then calculated from the selected compensation power by inverse Clark transformer.

$$i_{ci}^* = \frac{1}{v_{ic}^2 + v_{icd}^2} \begin{bmatrix} v_{ic} & v_{icd} \end{bmatrix} \begin{bmatrix} p_{ci} \\ q_{ci} \end{bmatrix} \quad i = a, b \quad (23)$$

Finally, the trigger signals for IGBT switches are then achieved by hysteresis pulse width modulation (PWM). More details about the HPQC compensation control system can also be found in [22, 24].

### 4 Simulation Results

Simulation verification using MATLAB/Simulink is

**Table 1** Co-phase traction system parameters.

Parameter	Value	Unit
Grid short-circuit level	1000	MVA
V/v trans. primary voltages	110	kV
V/v trans. secondary voltages	27.5 , 13.75	kV
V/v trans. nominal power	2 × 31.5	MVA
DC-link capacitance ( $C_{dc}$ )	10	mF
DC-link ref. voltage ( $V_{dc}$ )	31.5	kV
Filter capacitance ( $C_m$ )	9.1734	$\mu$ F
Filter capacitance ( $C_n$ )	4.97	mF
Filter inductance ( $L_n$ )	2.038	mH
Filter resistance ( $R_n$ )	40	$\Omega$
capacitance ( $C_c$ )	84	$\mu$ F
inductance ( $L_a$ )	10.9	mH
inductances ( $L_b$ )	4	mH
$k_p$ and $k_i$ via T&E method	15 and 6	-
$k_p$ and $k_i$ via G.A optimization	9.75 and 16.64	-

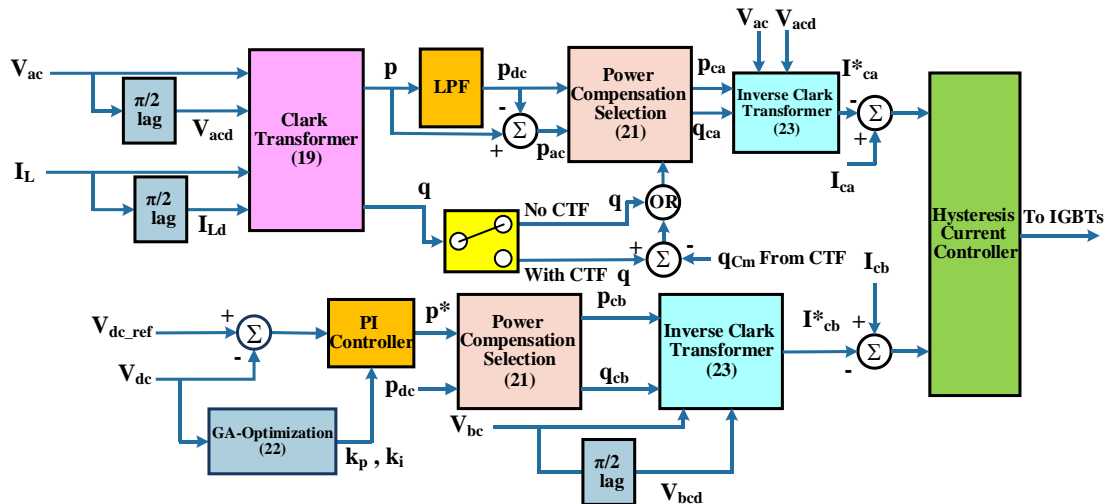


**Fig. 5** System control block diagram of the HPQC.

**Table 2** Loading sequences and simulation results of case studies.

Case	Intervals	Mode	$r$ [p.u.]	$PF_L$	$PF_G$	THD [%]	NSC [%]	$S_{HPQC}$ [MVA]	Reduction [%]
Case 1	$0.1 \leq t \leq 0.2$	No Filter	1	0.85	0.73	15.52	99		
	$0.2 \leq t \leq 0.3$	With Filter			0.81	15.03			
Case 2	$0.1 \leq t \leq 0.2$	No Filter	1	0.85	0.73	15.52	1.45	13.78	
	$0.2 \leq t \leq 0.3$	With Filter			0.99	2.81			
Case 3	$0 \leq t \leq 0.5$	With Filter, T&E	1.5	0.85	0.99	3.72	1.56	18.09	
	$0 \leq t \leq 0.5$	With Filter, G.A							

performed to show the reduction of the HPQC capacity and improved DC-link voltage performance. The input system parameters which is considered in the simulation are listed in Table 1. The traction loads are taken into consideration as varying harmonic loads simulated using rectifier RL load. Three cases of different loading are studied to compare the performance of the HPQC, as listed in Table 2.

The rated traction load is assumed to be 10 MVA (1 p.u.) for one unit train, which is defined as  $r$ . The simulation results are shown in Table 2 and Figs. 6-8.

The co-phase traction performance without the HPQC is initially analyzed in case 1, while the C-type filter is applied at 0.2 s. In Fig. 6, the three-phase voltage and current source are shown. Despite the improvement of the grid PF (from 0.73 to 0.81) and current distortion THD (from 15.52% to 15.03%) by the C-type filter, the NSC index would be remained 99%, and system exceeds its power quality limits and should be compensated by the HPQC. In case 2, the HPQC is initialized to compensate current unbalance, reactive power, and harmonics problems. Two loading

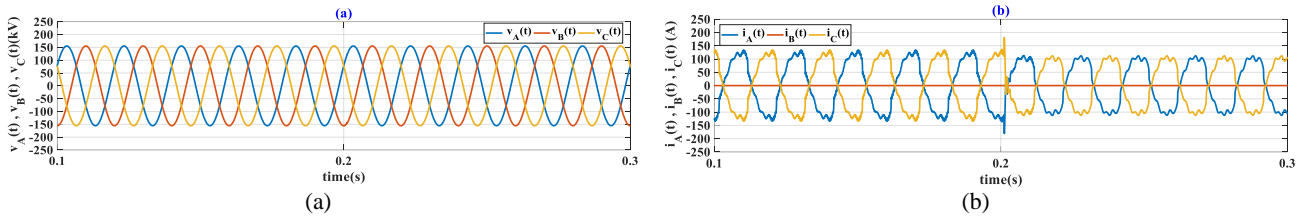


**Fig. 6** Co-phase traction system with C-type filter and without the HPQC: a) Three-phase grid voltage and b) Three-phase grid current.

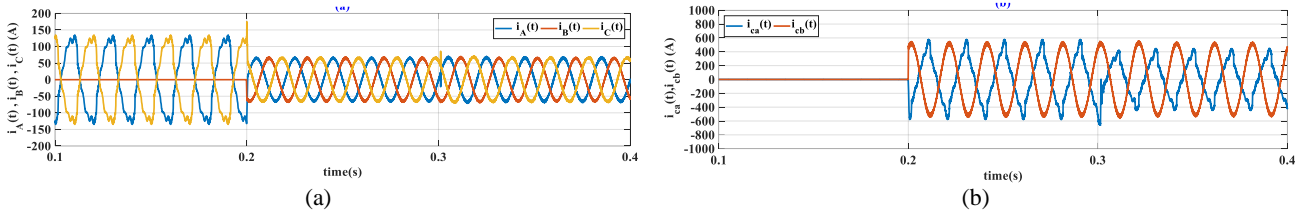


**Fig. 7** Co-phase traction system with the HPQC and C-type filter in FC method: a) three-phase grid currents and b) compensation currents.

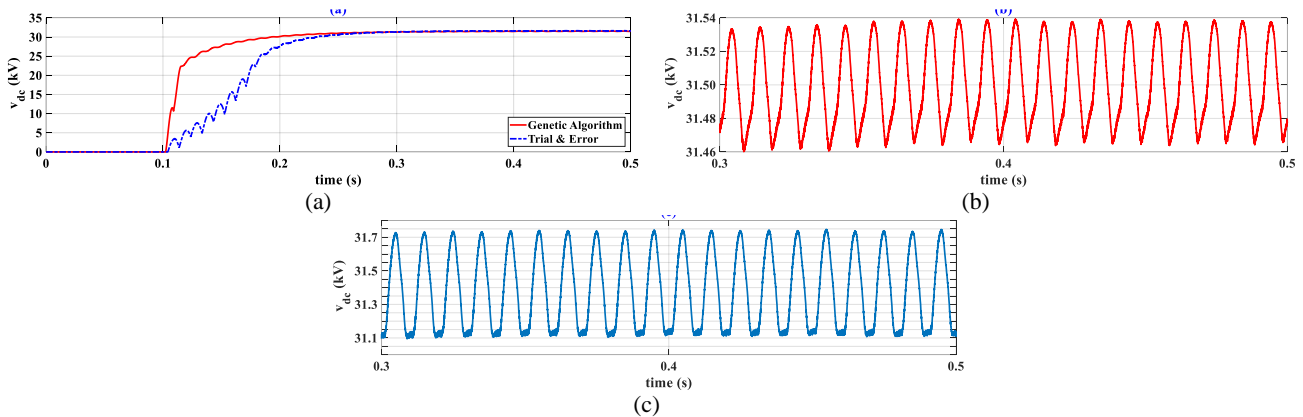


**Fig. 8** DC-link voltage: a) rise time for both T&E and G.A, b) peak to peak for G.A optimization, and c) peak to peak for T&E design.

conditions (1 and 1.5 p.u.) are considered with and without the filter in FC method, which its simulation results are tabulated in Table 2.

For case 2, the HPQC and the C-type filter are applied to the system with rated traction load (10 MVA) at 0.2 s and 0.3 s, respectively. Three-phase current waveforms are illustrated in Fig. 7(a). As can be seen, the grid currents are symmetric free-harmonic currents after using HPQC. The improvement of grid PF (from 0.73 to 0.99), current THD (from 15.52% to 3.29%), and NSC (from 99% to 1.45%) are obtained by the HPQC. In addition, the current THD is further improved by the C-type filter (from 3.29% to 2.81%), resulting in high-order harmonics mitigation. As shown in Fig 7(b),  $I_{ca}$  decreases while  $I_{cb}$  stays constant by applying the C-type filter. Therefore, the total compensation currents are reduced, and the rating of the HPQC capacity is diminished in the same voltage operation, which conforms previous theoretical studies. 18.86% reduction of the HPQC capacity is achievable via the C-type filter compared to the conventional configuration for rated traction load. In case 3, the 15 MVA traction load is

simulated for both T&E and G.A methods by using both HPQC and C-type filter applied at 0.1 s. The corresponding DC-link voltages are depicted in Fig. 8. As can be seen, with G.A optimization, the DC-link voltage has a faster dynamic response compared to T&E method (Fig. 8(a)). The maximum peak to peak DC-link voltage has been optimized from 600 V (via T&E method) to 80 V (via G.A optimization), as shown in Figs. 8(c) and 8(b), respectively. Besides, with the optimized performance of the DC-link voltage via G.A, the better power quality parameters would be expected, as listed in Table 2.

### 5 Conclusion

In this paper, the C-type filter design is investigated in the co-phase traction system for the capacity reduction of the HPQC. Mathematical studies are conducted to evaluate the usefulness of the C-type filter in the FC method. Unlike other methods, the proposed configuration does not need any change in the control system. Therefore, this structure may be used to reduce the size, the installation cost of the HPQC as well as to

mitigate high-order harmonics in the co-phase traction system. It is verified through simulation results that the 18.86% reduction of the HPQC rating is fulfilled with the C-type filter for the rated load. Eventually, the HPQC is simulated via G.A optimization for 1.5 p.u. traction load. The simulation results show the satisfactory performance of the DC-link voltage.

## References

- [1] A. T. Langerudy, A. Mariscotti, and M. A. Abolhassani, "Power quality conditioning in railway electrification: a comparative study," *IEEE Transactions on Vehicular Technology*, Vol. 66, No. 8, pp. 6653–6662, 2017.
- [2] S. M. M. Gazafrudi, A. Tabakhpour Langerudy, E. F. Fuchs, and K. Al-Haddad, "Power quality issues in railway electrification: A comprehensive perspective," *IEEE Transactions on Industrial Electronics*, Vol. 62, No. 5, pp. 3081–3090, 2015.
- [3] H. M. Roudsari, S. Jamali, and A. Jalilian, "Dynamic modeling, control design and stability analysis of railway active power quality conditioner," *Electric Power Systems Research*, Vol. 160, pp. 71–88, 2018.
- [4] H. M. Roudsari, A. Jalilian, and S. Jamali, "Flexible fractional compensating mode for railway static power conditioner in a V/v traction power supply system," *IEEE Transactions on Industrial Electronics*, Vol. 65, No. 10, pp. 7963–7974, 2018.
- [5] H. M. Roudsari, A. Jalilian, and S. Jamali, "Hybrid railway power quality conditioner based on half-bridge converter and asymmetric balanced traction transformer with deadbeat current control," *IET Power Electronics*, Vol. 12, No. 13, pp. 3447–3459, 2019.
- [6] B. Xie, Z. Zhang, S. Hu, Y. Li, L. Luo, and S. Sun, "YN/VD connected balance transformer-based electrical railway negative sequence current compensation system with passive control scheme," *IET Power Electronics*, Vol. 9, No. 10, pp. 2044–2051, 2016.
- [7] S. Hu, Y. Li, B. Xie, M. Chen, Z. Zhang, L. Luo, Y. Cao, A. Kubis, and C. Rehtanz, "A YD multifunction balance transformer-based power quality control system for single-phase power supply system," *IEEE Transactions on Industry Applications*, Vol. 52, No. 2, pp. 1270–1279, 2016.
- [8] F. Ciccarelli, M. Fantauzzi, D. Lauria, and R. Rizzo, "Special transformers arrangement for AC railway systems," in *Electrical Systems for Aircraft, Railway and Ship Propulsion (ESARS)*, pp. 1–6, 2012.
- [9] A. G. Lange and G. Redlarski, "Selection of C-type filters for reactive power compensation and filtration of higher harmonics injected into the transmission system by arc furnaces," *Energies*, Vol. 13, No. 9, p. 2330, 2020.
- [10] M. Habibolahzadeh, H. M. Roudsari, A. Jalilian, and S. Jamali, "Improved railway static power conditioner using c-type filter in scott co-phase traction power supply system," in *10<sup>th</sup> International Power Electronics, Drive Systems and Technologies Conference (PEDSTC)*, Shiraz, Iran, pp. 355–360, 2019.
- [11] H. Hu, Z. He, and S. Gao, "Passive filter design for china high-speed railway with considering harmonic resonance and characteristic harmonics," *IEEE Transactions on Power Delivery*, Vol. 30, No. 1, pp. 505–514, 2015.
- [12] S. K. M. Kodsai, C. A. Cañizares, and M. Kazerani, "Reactive current control through SVC for load power factor correction," *Electric Power Systems Research*, Vol. 76, No. 9–10, pp. 701–708, 2006.
- [13] Z. Qiuhaio, L. Guohui, and P. Yu, "Control method of STATCOM for electric railway," in *World Automation Congress (WAC)*, pp. 1–4, 2012.
- [14] V. P. Joseph and J. Thomas, "Power quality improvement of AC railway traction using railway static power conditioner a comparative study," in *International Conference on Power Signals Control and Computations (EPSCICON)*, pp. 1–6, 2014.
- [15] T. Tanaka, N. Ishikura, and E. Hiraki, "A novel simple control method of an active power quality compensator used in electrified railways with constant DC voltage control," in *Industrial Electronics (IECON)*, pp. 502–507, 2008.
- [16] F. Ma, A. Luo, X. Xu, H. Xiao, C. Wu, and W. Wang, "A simplified power conditioner based on half-bridge converter for high-speed railway system," *IEEE Transactions on Industrial Electronics*, Vol. 60, No. 2, pp. 728–738, 2013.
- [17] K. Lao, N. Dai, W. Liu, and M. Wong, "Hybrid power quality compensator with minimum DC operation voltage design for high-speed traction power systems," *IEEE Transactions on Power Electronics*, Vol. 28, No. 4, pp. 2024–2036, 2013.
- [18] A. Ghassemi, S. S. Fazel, I. Maghsoud, and S. Farshad, "Comprehensive study on the power rating of a railway power conditioner using thyristor switched capacitor," *IET Electrical Systems in Transportation*, Vol. 4, No. 4, pp. 97–106, 2014.



- [19] B. Chen, C. Zhang, W. Zeng, G. Xue, C. Tian, and J. Yuan, "Electrical magnetic hybrid power quality compensation system for V/V traction power supply system," *IET Power Electronics*, Vol. 9, No. 1, pp. 62–70, 2016.
- [20] A. T. Langerudy and S. M. M. G, "Hybrid railway power quality conditioner for high-capacity traction substation with auto-tuned DC-link controller," *IET Electrical Systems in Transportation*, Vol. 6, No. 3, pp. 207–214, 2016.
- [21] K. W. Lao, M. C. Wong, N. Y. Dai, C. S. Lam, L. Wang, and C. K. Wong, "Analysis in the effects of operation voltage range in flexible DC control on railway HPQC compensation capability in high-speed co-phase railway power," *IEEE Transactions on Power Electronics*, Vol. 33, No. 2, pp. 1760–1774, 2017.
- [22] N. Y. Dai, K. W. Lao, M. C. Wong, and C. K. Wong, "Hybrid power quality conditioner for co-phase power supply system in electrified railway," *IET Power Electronics*, Vol. 5, No. 7, pp. 1084–1094, 2012.
- [23] M. Habibolahzadeh, H. M. Roudsari, A. Jalilian, and S. Jamali, "Hybrid SVC-HPQC scheme with partial compensation technique in co-phase electric railway system," in *27<sup>th</sup> Iranian Conference on Electrical Engineering (ICEE)*, Yazd, Iran, pp. 679–684, 2019.
- [24] K. Lao, M. Wong, N. Dai, C. Lam, C. Wong, and L. Wang, "Analysis in the effect of co-phase traction railway HPQC coupled impedance on its compensation capability and impedance-mapping design technique based on required compensation capability for reduction in operation voltage," *IEEE Transactions on Power Electronics*, Vol. 32, No. 4, pp. 2631–2646, 2017.
- [25] X. Xu, B. Chen, and F. Gan, "Electrical railway active power filter research based on genetic algorithms," in *International Conference on Control and Automation*, pp. 1465–1468, 2007.

- [26] B. Xie, Y. Li, Z. Zhang, S. Hu, Z. Zhang, L. Luo, et al., "A compensation system for co-phase high-speed electric railways by reactive power generation of SHC&SAC," *IEEE Transactions on Industrial Electronics*, Vol. 65, No. 4, pp. 2956–2966, 2017.



**M. Habibolahzadeh** was born in Tehran, Iran, in 1988. He received the B.Sc. degree in Electrical Engineering from Islamic Azad University, Tabriz Branch, Tabriz, Iran, in 2012, and the M.Sc. degree in Electrical Engineering, Power Electronics, and Electric Machines from Iran University of Science and Technology (IUST), Tehran, Iran, in 2018. His employment experience included the Tehran Regional Electric Company (TREC), and Alborz Construction Engineering Organization (ACEO). His special fields of interest included power quality, power electronic converters, and electric railway systems.



**A. Jalilian** was born in Yazd, Iran in 1961. He received the B.Sc. degree in Electrical Engineering from Iran, in 1989, the M.Sc. and the Ph.D. degrees in Electrical Engineering from Australia, in 1992, and 1997, respectively. He joined the power group of the School of Electrical Engineering at Iran University of Science and Technology (IUST) in 1998, where he is a Professor. Prof. Jalilian is a member of the Centre of Excellence for Power System Automation and Operation at IUST. He is also head of Power Quality Laboratory at IUST where he has supervised B.Sc., M.Sc., and Ph.D. research students in different projects mostly in the area of electric power quality. His research interests are causes, effects, and mitigation of power quality problems in electrical systems, and microgrids. Since 1997, Prof. Jalilian Has been a reviewer for several IEEE Transactions, IET, and Elsevier journals, and a member of the technical committee of several national, and international conferences.



© 2021 by the authors. Licensee IUST, Tehran, Iran. This article is an open access article distributed under the terms and conditions of the Creative Commons Attribution-NonCommercial 4.0 International (CC BY-NC 4.0) license (<https://creativecommons.org/licenses/by-nc/4.0/>).